Department of Chemical Engineering

University of Wisconsin-Madison

Madison, Wisconsin

CBE424: Operations and Process Laboratory

Heat transfer modelling in single-pass one tube and two shells heat exchanger model

Supervisor: Doctor Jimenez

Khoa Nguyen Bui

Partner: Abdullah Alkazrai

Date completed: 8/10/2022

Date submitted: 8/10/2022

Abstracts

Accurate heat transfer modeling of unusual heat transfer designs is crucial in all industries for energy consumption planning and management. For this report, a single-pass tube with modification of two shells heat exchanger was built. The relationship between the tube-side flowrate versus the overall heat transfer coefficients of the tube-side, Ui,1, and first shell, Ui,2, were studied. Mathematical equations of conventional single-pass, tube-and-shell heat exchangers were proposed to model the relationship. Seven faucet settings at the tube-side stream, which correspond to seven flowrate settings, were tested. Out of these, two flowrate settings were above 0.015 kg/s, and five flowrate settings were below 0.015 kg/s. Both shells' flow rates were kept the same throughout all trials. The resulting $U_{i,1}$ and $U_{i,2}$ calculated from experimental data did not follow consistent trends. The grouped $U_{i,1}$ and $U_{i,2}$ data with their respective mass velocities range had errors up to 8 times higher than the confidence interval of 5% standard deviation, indicating poorly replicated data. The inaccurate data led to an average % difference of 67.5 ± 39.2 % and 53.0 ± 42.0 % between the calculated and the model prediction of $U_{i,1}$ and $U_{i,2}$ respectively. In conclusion, the relationship between tube side flowrates and $U_{i,1}$ and $U_{i,2}$ for single-pass tubes with two shells heat exchangers could not be modeled due to data inconsistency. This result was attributed to many design problems, such as lack of insulation over the system, short tube length, and lack of control over shell-side flowrates.

Table of Contents

Background

Energy consumption is one of the main production costs in the industrial process, reaching an average monthly bill of $5,370 for factories in the U.S (Analysts, 2021). Across all factories, this monthly bill could total up to $200 billion annually (Constellation, n.d.). However, 52% of the consumed energy is wasted due to inefficient designs and management, leading to high, unnecessary energy costs (Constellation, n.d.). Most energy is used for heat-related phenomena, such as process heating, co-generation, industrial boiler, and heat exchanger. Hence, being able to apply basic heat transfer concepts studied onto a lab-scale prototype of a more complex heat exchange model can lower the industry's expenditures on energy. In this report, we design a modified, counter-current, tube-and-shell heat exchanger to study the correlation between the flowing fluid's mass velocity and the overall heat transfer coefficient in the system.

All the model introduced for this experiment were consulted from the Heat Transfer section of the CBE 424: Laboratory Manual (Heat Exchanger Experiment). In a single pass tube-and-shell system, most heat exchangers are modeled using Newton's Law of Cooling, represented by Equation 1 below:

$$U = \frac{Q}{A_L \Delta T_{LM}} \quad \text{(Eq. 1)}$$

Here, U is the overall heat transfer coefficient, $A_L = \pi DL$ is the area of heat transfer in the tube, ΔT_{LM} is the log-mean temperature difference, and $Q = wC_p(T_{out} - T_{in})$ is the heat rate transferred by relevant fluid stream. For an ideal counter-current orientation, ΔT_{LM} is define as:

$$\Delta T_{LM} = \frac{(T_{h,in} - T_{c,out}) - (T_{h,out} - T_{c,in})}{\ln \frac{(T_{h,in} - T_{c,out})}{(T_{h,out} - T_{c,in})}} \quad \text{(Eq. 2)}$$

Where T is temperature with lower suffix *h* and *c* to indicate hot and cold streams, and lower suffix *in* and *out* for inlet and outlet temperature. These temperature and mass flowrate

measurements could be collected to determine the experimental heat transfer coefficient U.

To make a predictive model of heat transfer coefficient U, another relationship was established which considers individual heat transfer resistance. However, the designed heat exchanger has a single tube encased in two shells. For model clarity, lower suffixes 1, 2, and 3 refer to the first tube, first shell, and second shell respectively, instead of suffixes h and c. Currently, there is no known tube-and-shell model of this prototype to my knowledge. However, single-pass tube-and-shell heat exchanger models could be modified for this heat exchanger design. Despite the design difference, $U_{i,1}$ could be calculated from the first tube and first shell. Then, the first tube and shell could be grouped as an overall tube, and $U_{i,2}$ could be calculated from the "overall" tube and second shell.

Usually, the single pass tube-and-shell model has well-established correlations for heat transfer coefficients, h, and thermal conductivity, k. However, they require specific heat exchanger designs. For example, the Kern model would require a triangle-pitch tube arrangement inside the shell, or Sieder-Tate requires smooth cylindrical tubes. Furthermore, these models assume a well-insulated system and temperature-independent materials. In a practical laboratory setting, there isn't sufficient equipment to build a heat exchanger that satisfies these conditions. Thus, the predictive model is simplified into Equation 3:

$$\frac{1}{U_{i,1}} = \left(\frac{a}{G_1^b} + c + \frac{d}{G_2^e}\right) \qquad \text{(Eq. 3)}$$

Where a, b, c, d, e are parameters to be determined from experimental data, and G_1 and G_2 are the mass velocity $G = \frac{w}{\pi N_T R^2}$ of first tube and first shell. The surrounding effects on the system can be generalized into these constants. Since $U_{i,1}$ already include the mass velocities of

first tube and shell flows, Equation 3 is modified into Equation 4 below to finds the overall heat transfer of the first shell-side, $U_{i,2}$:

$$\frac{1}{U_{i,2}} = \left(\frac{a_1}{U_{i,1}^{b_1}} + c_1 + \frac{d_1}{G_3^{e_1}} \right) \quad \text{(Eq. 4)}$$

Where a, b, c, d, and e with suffix 1 is another set of parameters to be determined, and G_3 is the mass velocity of the second shell. An advantage of these parameters are factors, such as area ratio $\frac{A_o}{A_i}$ when heat transfer coefficient of the inner wall gets related to shell side, would be accounted for appropriately by all the determined constants. Thus, both Equations 3 and 4 only require the assumption of heat transfer in material to be independent of temperatures.

The experimental $U_{i,1}$ and $U_{i,2}$ is calculated using Equation 1 and 2, and these results would fit into Equation 3 and 4 simultaneously for model $U_{i,1}$ and $U_{i,2}$. From these models, we expected an exponential relationship where increasing flow rate would lower heat resistance and increase both heat transfer coefficient values.

Experimental Design

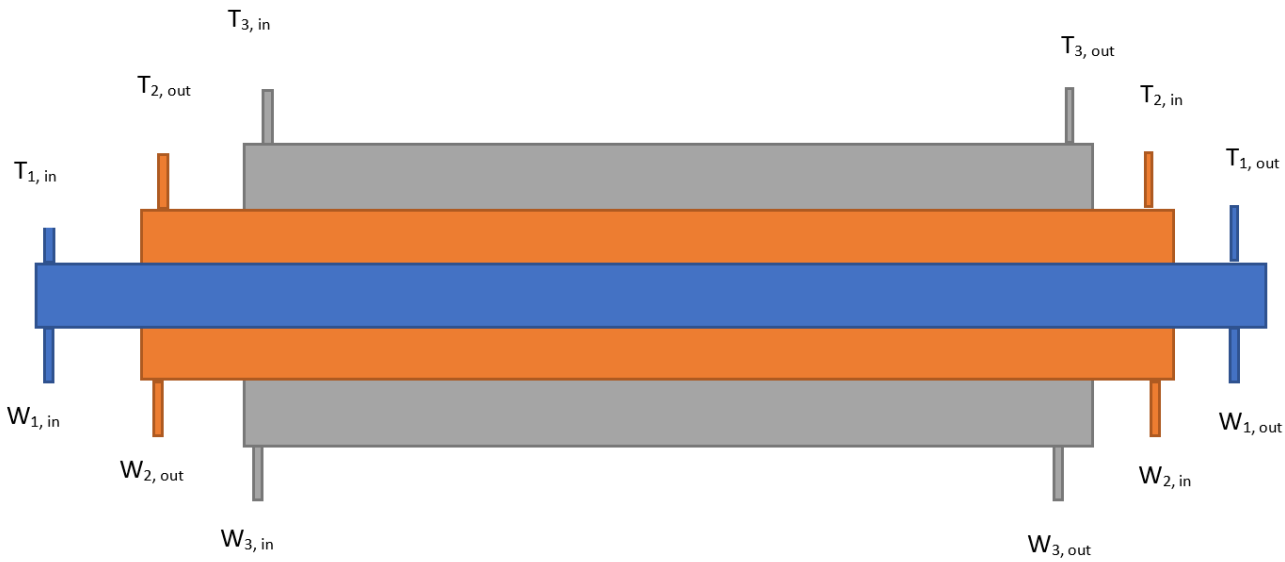

The single pass 1-tube-2-shells heat exchanger was constructed following the schematic in figure 1. All tubes and shells were made of PVC pipes. For the inner tube, first shell, and second shell, their lengths were 12, 18, and 24 in, their inner diameters were 0.0153, 0.0258, and 0.0398 in, and their outer diameters were 0.0214, 0.0334, and 0.0483 in. At each end of the tubes and shells, a small hole and a large hole were drilled to fit a thermocouple sensor and hose barbed fitting respectively. In total, 6 temperatures sensor were used to measure the inlet and outlet of each tube and shell fluid temperature. The barbed fittings were for fitting rubber tubes, which introduced fluid on one end and allowed it to escape to the other end.

The first shell ran counter-current to the first tube and the second shell to model the counter-current heat exchanger. For the two shells, the inlet barbed fittings ran tubes from a heated water bath pump, one pump for each shell, through a three-ways control valve. This allowed us to switch between directing water for pump self-circulation during heating and

directing water through the heat exchanger. These water-bath pumps only ran at a constant flow rate. For the first tube side of the heat exchanger, the inlet fits a rubber tube to a sink faucet. The tube flow rate was controlled by partially opening the faucet. All outlets' barbed fittings had tubes leading to the sink to dispose of the flowing water.

The experiment was initiated by filling both pumps with DI water for heating. The temperature set for the first and second shell pumps were 51 and 60 ^{o}C, respectively. During heating, the three-way valves were turned for both pumps to self-circulate, and the tube water stream was introduced through the heat exchanger by turning on the faucet. While the water pumps were heating, the mass flow rate of the tube stream could be measured using a beaker and a stopwatch. The faucet stream was controlled to output a flowrate below 50 g/second, a speed comparable to the pump rates of the two water bath pumps. Once the water bath reached their respective temperature, both three-way valves were turned to run hot water through the first and second shells. The system was allowed to reach a steady state. Meanwhile, both shells' mass flow rates were measured using a beaker and a stopwatch. The measurement was done only once for both pumps as they pumped at a constant, unchangeable flow rate. Once the heat exchanger reached a steady state of constant temperature at the inlets and outlets, all relevant temperatures were recorded. The water bath pumps were put into self-circulation again and re-filled with water for the next run.

This setup was performed for 7 different tube stream faucet setting, with 5 trials for each setting at low flow speed below 0.015 kg/s and 2 trials for high flow speed above 0.015 kg/s. The mass flowrate and temperature collected was used to calculate experimental $U_{i,1}$ and $U_{i,2}$. Then, these values were fit into Equation 3 and 4 through performing Sum Squared Errors.

Result and Discussion

The resulting $U_{i,1}$ and $U_{i,2}$ calculated and modeled were plotted against the mass velocity of tube-side stream in Figures 1 and 2. Overall, a poor exponential relationship was observed between increasing the tube-side flowrate to increasing overall heat transfer coefficient $U_{i,1}$ and $U_{i,2}$. For both models, the $U_{i,1}$ and $U_{i,2}$ experimental values fluctuated greatly for mass velocity below 0.04 kg/in^{2}s. For example, $U_{i,1}$ fluctuated between 0.0185 to 0.0253 J/ (s in^2 K) and $U_{i,2}$ fluctuated between 0.019 to 0.141 J/ (s in^2 K) for mass velocities range from 0.007 to 0.01 kg/ in^{2}s. This fluctuation impacted the model fitting accuracy. Furthermore, the inaccurate data also made it difficult to qualitatively identify outliers, which impacted the ability to determine the precise $U_{i,1}$ and $U_{i,2}$ values at each mass velocity range. On average, all experimental data had up to 67.5 ± 39.2 % and 53.0 ± 42.0 % difference from the model prediction for $U_{i,1}$ and $U_{i,2}$, respectively. Thus, using these calculated data to predict accurate parameters for Equations 3 and 4 became unfeasible.

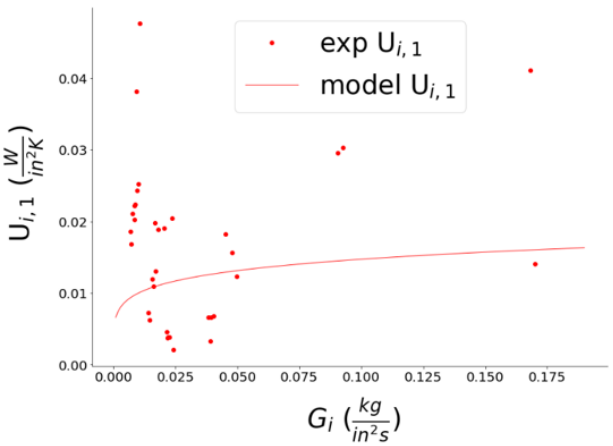

Figure 1. The heat transferred coefficient of $U_{i,1}$ plotted against mass velocity G_i. Experimental $U_{i,1}$ (red dot) and Equation 3 (red line) model $U_{i,1}$

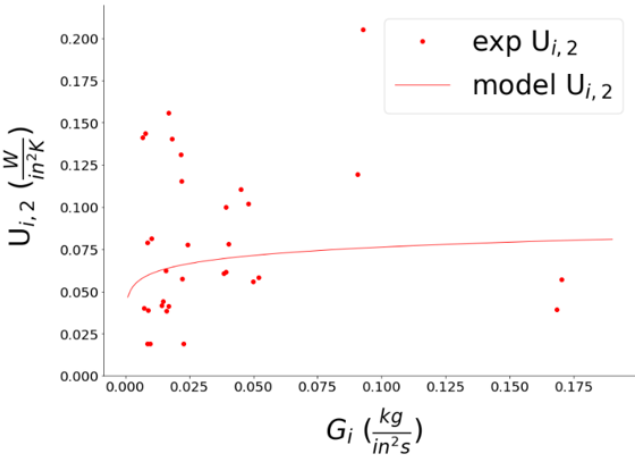

Figure 2. The heat transferred coefficient of $U_{i,2}$ plotted against mass velocity G_i. Experimental $U_{i,2}$ (red dot) and Equation 4 (red line) model $U_{i,2}$.

The high fluctuation between all data within the same mass velocity range also portrayed unreliable replication of trial runs. The averaged $U_{i,1}$ and $U_{i,2}$ for the 5 faucet settings below the flowrate of 0.015 kg/s were summarized into four mass flowrate ranges in Table 1. All the standard deviation values for the calculated $U_{i,1}$ and $U_{i,2}$ were 1 to 8 times higher than the confidence interval of 5% standard deviation. As a result, not only were the parameter fittings for Equations 3 and 4 unfeasible, but they were also unreliable due to poor replication consistency. The lack of accurate, reliable data introduced multiple combinations of parameter possibilities for Equations 3 and 4. Constraints could be introduced onto all parameters to narrow down parameters' possibilities. However, this became difficult for an unusual heat exchanger design with no prior data or model to narrow the constraints.

Table 1. Chosen mass velocity ranges and their corresponding average, standard deviation, and standard deviation % of heat transfer coefficient $U_{i,1}$ and $U_{i,2}$. All standard deviation % at above standard 5% confidence intervals, indicating replications are unreliable.

Mass velocity range G_i ($\frac{kg}{s}$)	Heat transfer coefficient $U_{i,1}$ ($\frac{W}{in^2K}$)			Heat transfer coefficient $U_{i,2}$ ($\frac{W}{in^2K}$)		
	Average	Standard deviation	Standard deviation %	Average	Standard deviation	Standard deviation %
0.006 - 0.011	0.0244	0.0067	27.6	0.0673	0.0496	73.7
0.014 – 0.017	0.0285	0.0073	25.5	0.0157	0.0027	17.5
0.021 – 0.025	0.0093	0.0024	26.1	0.0353	0.0238	67.5
0.038 – 0.041	0.0208	0.0052	25.1	0.0211	0.0046	21.8

The inconsistencies in the data collection process were attributed to multiple experimental setup problems. We set up the thermocouples by inserting the sensor through the tube wall to measure the water temperature flowing inside the shell. The fluid area between each

layer was small, leading to a high chance of thermocouples touching the inner layer tube walls instead. Also, flowing fluids impacted the sensitivity of the sensor, leading it to fluctuate consistently between ± 0.2 ^{o}C. As a result, the thermocouples fluctuated consistently and may be measuring tube and shell wall temperature instead of water temperature. Coupled with the resulting inlet and outlet temperature changing by only 0.3-0.4 ^{o}C, we often ended up with temperature fluctuations that were not possible, including the cold inlet stream further being cooled by the hot stream.

Another setup problem was the lack of control over the flow rates of all water streams. Only the tube-side flow rate could be controlled by a faucet, which depended on how far the tap was open qualitatively. Even then, since the faucet was part of the lab's water system, the output of the faucet flow varied randomly, depending on other people using other sinks and water outlets. There was a possibility that our flow rate fluctuated during each trial run due to this problem. Furthermore, the cold tube stream was limited to a flow rate 5 to 10 times smaller than hot-stream flow rates. Both hot flow rates ran at 0.023 and 0.021 kg/s for the first and second shells, respectively. Running the tube stream at this flow rate resulted in a small temperature change of ± 0.1-0.2 ^{o}C between its inlet and outlet stream. Combining this observation with the thermocouples sensitivity problem, any results collected for tube stream flow rate above 0.02 kg/s were considered highly inaccurate and imprecise. This would be reflected in the 4 data points collected above mass velocities of 100 kg/ in^2 s in Figures 1 and 2.

Additional design consideration was it lacked length and surface area for heat transfer capacity. We assumed a small, short heat exchanger would be sufficient to observe a strong exchange capacity. However, many known heat tube-and-shell heat exchangers were designed with multiple tubes passing within a shell. For instance, CBE 424 lab tube-and-shell heat

exchangers have 31 tubes within a shell. This design exposed more surface area of tube flow to the shell stream, which improved heat exchanging capacity. Since our heat exchanger only has one tube within one shell, the heat transfer availability was poor compared to the lab design. As a result, a temperature change of only ± 0.3 ^{o}C between all streams was achieved for our heat exchanger design.

Finally, the biggest limitation to our design that we overlooked was the lack of insulation. This led to the outermost shell losing heat to the surroundings instead of directing its energy transfer toward the inner shell. The outer shell, on average, has a heat rate of 15.6 times higher than the cold tube stream. This meant that the heat exchanged between the system was smaller than the heat loss to the system. As a result, the design wasted much energy that could have been transferred inward and improved the collected data by allowing for more heat to be exchanged.

Conclusion and Recommendations

Overall, the proposed models in Equations 4 and 5 correlated poorly with the experimental data of the one tube-to-two-shells heat exchanger. The experimental data had an average difference of 67.5 ± 39.2 % and 53.0 ± 42.0 % between the calculated and the model prediction of $U_{i,1}$ and $U_{i,2}$, respectively. The large errors observed were due to poor replicates of data points, as the average mass velocities range and its corresponding averaged $U_{i,1}$ and $U_{i,2}$ all had standard deviations of up to 8 times higher than the confidence interval of 5%. As a result, it was unclear whether Equation 4 or 5 would be viable models for the heat transfer design studied in this report, as the data collected were imprecise and inconsistent.

Multiple problems with the heat exchanger design were identified for future improvements and studies. Adding insulation surrounding the heat exchanger would improve the driving force of heat transfer inward the tubes. Building an extended system, such as doubling the tube, first shell, and second shell lengths to 48, 44, and 40, would allow for more heat transfer surface area. Three-ways valves that control and lower the hot flowrate streams could be bought and used for the same pumps. An extra pump could be introduced for the inlet tube instead of using a faucet for more consistent temperature and flow rate control. These improvements should theoretically allow for larger temperature change between all streams, allowing for better replications of results. More thermocouples could also be used to measure the outlet and inlet temperature of just the water stream once exited the system. Introducing valves that may change flow rates too would allow for more flow rate conditions to be tested.

To conclude, while the experiment resulted in a poor outcome, it gave insights into the challenges faced when designing an unusual heat exchanger and attempting to build

mathematical models for the system. During the experimental process, we were focused on deriving a mathematical equation suitable for modeling the heat exchanger studied in this report. However, the inconsistencies of the data generated made us realize the importance of also considering the practical constraints. This experiment showed us that being able to derive equation models for a system became obsolete if the design itself could not perform consistently to verify them. Therefore, it is important to understand and identify aspects of the experiment design that could be improved to generate more consistent and reliable data.

References

Analysts, P. C. (2021, 11 15). *Average Factory Electric Bill: How Much Should You Pay?* Retrieved from https://www.costanalysts.com/: https://www.costanalysts.com/average-factory-electric-bill/

Constellation. (n.d.). *6 Ways Manufacturers Can Reduce Industrial Energy Costs*. Retrieved from https://blogs.constellation.com/.

Energy, D. o. (2014, 9 17). *Energy Department Takes Major Steps to Increase U.S. Energy Productivity and Manufacturing*. Retrieved from energy.gov: https://www.energy.gov/articles/energy-department-takes-major-steps-increase-us-energy-productivity-and-manufacturing

(n.d.). *Heat Exchanger Experiment.* CBE 424 Lab Manual:.

Kevin M. Moroney, K. O.-J. (2019, July 31). *Analysing extraction uniformity from porous coffee beds using mathematical modelling and computational fluid dynamics approaches*. Retrieved from PLOS ONE: https://journals.plos.org/plosone/article?id=10.1371/journal.pone.0219906

Thiyam Tamphasana Devi, B. K. (2017). *Mass transfer and power characteristics of stirred tank with Rushton and curved blade impeller*. Retrieved from Engineering Science and Technology, an International Journal,Volume 20, Issue 2: https://www.sciencedirect.com/science/article/pii/S2215098616306413

Appendices

Table of collected data

Table 1: Table of all tube stream flowrate trials and their corresponding inlet and outlet temperature of all tube stream T_1, first shell T_2, and second shell T_3. All runs had first and second shell flowrates of 0.0229 and 0.0213 kg/s respectively. Tube stream flowrate was measured using bucket and stopwatch method, and their corresponding mass of water measured over time collected are included.

Run	mass water measured (kg)	Time collected (s)	Mass flowrate (kg/s)	T3,in	T3,out	T2, in	T2, out	T1,in	T1,out
1	0.1845	60.46	0.003052	59.8	57.3	41.1	49.6	24.2	27.4
2	0.1605	60.35	0.002659	59.5	57.3	44	49.4	24.2	27.4
3	0.3055	44.94	0.006798	59.9	56.9	39.6	49.4	25.3	25.9
4	0.2345	40.05	0.005855	59.9	57.9	41.6	49.8	25.1	25.8
5	0.207	40.04	0.00517	59.9	58.1	49.9	50.6	19.2	20.4
6	0.2405	50.23	0.004788	60	58.4	49.8	50.6	18.1	19.5
7	0.412	30.04	0.013715	60.1	58.6	50.5	51	18.1	18.5
8	0.392	30.41	0.01289	59.9	57.9	50.7	51.2	18	18.5
9	0.536	20.25	0.026469	60.4	58.7	50.5	51.5	18.5	18.9
10	0.5325	20.61	0.025837	60.4	59.2	50.7	51.3	18.5	18.9
11	0.4935	10.16	0.048573	60	59	50.4	50.1	18.3	18.4
12	0.4985	10.37	0.048071	60.4	59.1	50.7	50.9	18.2	18.5
13	0.148	60.43	0.002449	60.3	59.1	50.6	51	19.7	22.6
14	0.1345	60.41	0.002226	60.2	59	50.7	51.4	20.2	23.2
15	0.1175	60.31	0.001948	60.3	59.2	50.7	51.4	20.4	23.4
16	0.1175	40.34	0.002913	59.3	56.5	49.4	49	21.3	23.8

17	0.1235	45.28	0.002727	59.3	57.5	49.1	49.2	20.9	23.5
18	0.1155	45.44	0.002542	59.4	57.4	49.4	49.2	20.7	23.3
19	0.11	45.2	0.002434	59.4	57.5	49.3	49.2	21.4	23.8
20	0.084	40.54	0.002072	59.4	56.9	49.4	49.2	20.8	23.2
21	0.194	40.11	0.004837	59.3	56.5	49.4	49.2	18.1	19
22	0.209	45.29	0.004615	59.4	57.4	49.3	49.1	17.6	18.4
23	0.182	40.26	0.004521	59.3	56.5	49.5	49.2	17.5	18.4
24	0.19	45.28	0.004196	59.2	55.6	49.4	49.2	18.1	18.6
25	0.192	47.43	0.004048	59.5	56.2	49.4	49.2	18	18.6
26	0.211	30.35	0.006952	59.5	57.1	49.4	49	17.6	17.5
27	0.2285	35.39	0.006457	59.4	57.4	49.2	49.1	17.9	18.1
28	0.221	35.35	0.006252	59.4	57.2	49.4	48.8	18.1	18.3
29	0.258	40.63	0.00635	59.4	57.5	49.4	49.1	18.3	18.5
30	0.2475	40.02	0.006184	59.5	57.8	43.4	44.5	18.8	19
31	0.304	20.45	0.014866	59.5	57	49.3	49	18.1	18.4
32	0.2905	20.39	0.014247	59.6	57.8	49.4	49.1	18	18.3
33	0.2475	21.46	0.011533	59.5	57.2	49.5	49.1	18.1	17.9
34	0.262	23.43	0.011182	59.7	57.3	49.9	49.4	18.3	18.4
35	0.241	21.46	0.01123	59.5	57.2	49.9	49.6	18.3	18.5
36	0.225	20.49	0.010981	59.6	57.2	49.8	49.5	18.7	18.9

Sample Calculation

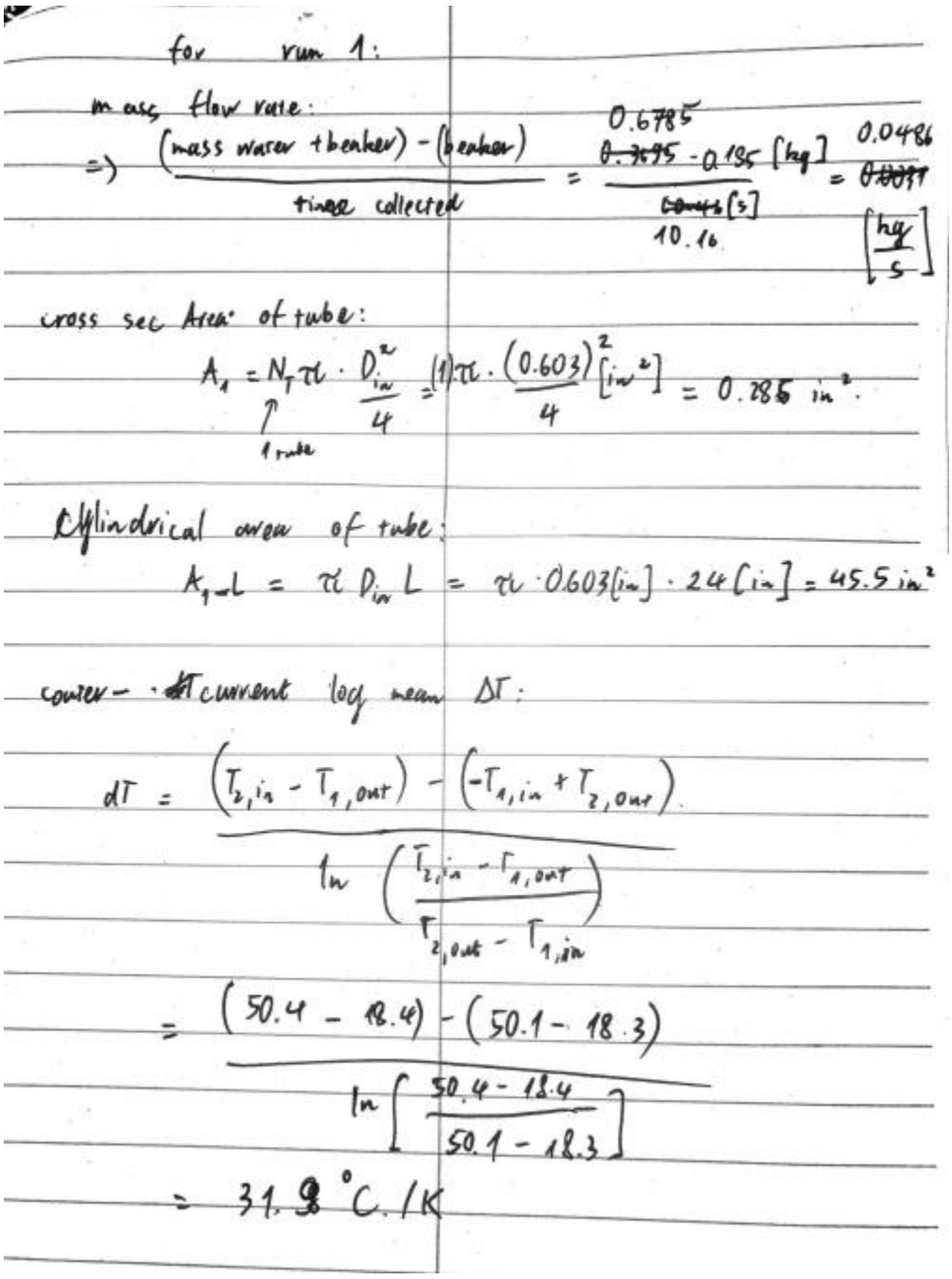

for run 1:

mass flow rate:

$$\Rightarrow \frac{(\text{mass water + beaker}) - (\text{beaker})}{\text{time collected}} = \frac{0.6785 - 0.185\ [kg]}{10.16\ [s]} = 0.0486 \left[\frac{kg}{s}\right]$$

cross sec Area of tube:

$$A_1 = \underbrace{N_T}_{1\ \text{tube}} \pi \cdot \frac{D_{in}^2}{4} = (1)\pi \cdot \frac{(0.603)^2}{4}\ [in^2] = 0.285\ in^2.$$

Cylindrical area of tube:

$$A_{1,L} = \pi D_{in} L = \pi \cdot 0.603[in] \cdot 24[in] = 45.5\ in^2$$

counter-current log mean ΔT:

$$dT = \frac{(T_{2,in} - T_{1,out}) - (-T_{1,in} + T_{2,out})}{\ln\left(\frac{T_{2,in} - T_{1,out}}{T_{2,out} - T_{1,in}}\right)}$$

$$= \frac{(50.4 - 18.4) - (50.1 - 18.3)}{\ln\left[\frac{50.4 - 18.4}{50.1 - 18.3}\right]}$$

$$= 31.9\ ^\circ C./K$$

Heat rate of tube 1:

$$Q = \dot{m} \cdot c_p \cdot (T_{1,out} - T_{1,in})$$

$$= 0.0486 \frac{kg}{s} \cdot 4200 \frac{J}{kg\,K} \cdot (18.4 - 18.3)\,K$$

$$= 20.4 \frac{J}{s}$$

Mass velocities $G_{i,1}$:

$$G_{i,1} = \frac{\dot{m}_1}{A_{cross}} = \frac{0.0486}{0.286} = 0.17 \left[\frac{kg}{in^2 s}\right]$$

$$\left[\frac{kg}{s}\right] \rightarrow \left[in^2\right]$$

Heat transfer coefficient $U_{1,in}$:

$$U_{1,in} = \frac{Q_1}{A_{1,L} \cdot \Delta T_1} = \frac{20.4\,J}{45.5\,in^2 \cdot 31.9\,K} = 0.0141 \left[\frac{J}{s\,in^2\,K}\right]$$

(can be done same step to find $U_{2,in}$)

but

$$\Delta T_2 = \frac{(T_{3,in} - T_{2,out}) - (T_{3,out} - T_{2,in})}{\ln\left(\frac{T_{3,in} - T_{2,out}}{T_{3,out} - T_{2,in}}\right)}$$

$$= 9.234\,K$$

and $Q_2 = w_2 C_p (T_{2,out} - T_{2,in})$

$= 0.0239 \frac{kg}{s} \cdot 4200 \frac{J}{kg\,K} \cdot (50.1 - 50.4)\,K$

$= -30.2 \frac{J}{s}$

& we make $|Q_2| = 30.2 \frac{J}{s}$

$V_{2-in} = \frac{Q_2}{A_{2,L} \cdot \Delta T_2} = \frac{30.2 \frac{J}{s}}{57.34\,in^2 \cdot 9.23\,K} = 0.057 \frac{J}{in^2\,s\,K}$

Average Group energy:

For G_i range $0.006 - 0.011 \frac{kg}{s}$

$V_{i,1\,exp} = [0.0185, 0.0211, 0.0232, 0.0253, 0.0262, 0.0222, 0.0203, 0.0195]$

Avg $V_{i,1} = 0.0244$ kg/s

Std $V_{i,1} = 0.0067$ kg/s

Std % $V_{i,1} \Rightarrow \frac{0.0067}{0.0244} \cdot 100 = 27.6\,\%$

Model $U_{i,1}$

$a = 80.737, 35$, $b = 0.2$, $c = 10.647$,

$d = 0.0097$, $e = 2.743$, $G_1 = 0.17$, $G_2 = 0.095$

$$= 0.0169 = 1 / \left[\frac{a}{G_1^{b}} + c + \frac{d}{G_2^{e}} \right]$$

$$= \left[\frac{J}{in^2 s K} \right]$$

Model $U_{i,2}$.

$a_1 = 0.449$ $b_1 = 0.74$, $c_1 = 2.4$, $d_1 = 0.24$,

$h_1 = 0.176$, & $U_{i,1} = 0.0169$, $G_3 = 0.037$

$$U_{i,2\,model} = 1 / \left[\frac{a_1}{U_{i,1\,mol}^{b_1}} + c_1 + \frac{d_1}{G_3^{e_1}} \right]$$

$$= 0.0826 \left[\frac{J}{in^2 s K} \right]$$

% dif : $U_{i,1}$: $\Rightarrow \frac{|U_{i,1} - U_{i,1\,model}|}{U_{i,1\,model}} \cdot 100 = 16.8\%$

$U_{i,2} \Rightarrow \frac{|U_{i,2} - U_{i,2\,model}|}{U_{i,2\,model}} \cdot 100 = 31.1\%$